

Heat Deposition of Erbium Lasers in Hard Dental Tissues



Tadej Perhavec^a, Matjaz Lukac^b, Janez Diaci^c, Marko Marincek^d

^a Graduate Student, University of Ljubljana, Faculty of Mechanical Engineering, Ljubljana, Slovenia.

^b Research Associate, Josef Štefan Institute, Light and Matter Department, Ljubljana, Slovenia.

^c Associate Professor of Mechatronics and Laser Applications, University of Ljubljana, Faculty of Mechanical Engineering, Ljubljana, Slovenia.

^d Research Associate, Josef Štefan Institute, Light and Matter Department, Ljubljana, Slovenia.

Purpose: The aim of this study was to determine residual heat deposition in hard dental tissues during ablation with Erbium lasers.

Materials and Methods: Residual heat deposition was obtained from measured irradiated hard tissue temperature decay characteristics immediately following Erbium laser pulses. A comparison of the heating effects of the two most commonly used Erbium lasers in laser dentistry, namely Er:YAG and Er,Cr:YSGG, was made.

Results: The measured residual heat was larger in enamel than in dentin for both laser sources. The amount of the unwanted residual heat that remains deposited in the tooth is for the H mode Er,Cr:YSGG laser twice as great, and for the S mode Er,Cr:YSGG laser more than 3 times as great as the deposited heat with the MSP mode Er:YAG laser.

Conclusion: For Er,Cr:YSGG lasers, a larger share of the total absorbed laser energy remained in the tooth in the form of heat. This explains, at least partially, the observed lower ablation efficacy of Er,Cr:YSGG lasers compared to Er:YAG lasers.

Keywords: Er:YAG, Er,Cr:YSGG, erbium laser, heat deposition, dental laser, hard dental tissues.

J Oral Laser Applications 2009; 9: 205-212.

Submitted for publication: 20.05.09; accepted for publication: 06.11.09.

Currently, two erbium laser wavelengths are most commonly used in dentistry: the Er:YAG (2940 nm) laser and the Er,Cr:YSGG (2780 nm) laser.¹ They exhibit the highest absorption of all infrared lasers in water and hydroxyapatite and are thus ideally suited for “optical drilling” in enamel, dentin and composite fillings.^{2,3} The Er:YAG laser has an approximately three times higher absorption in water compared to the Er,Cr:YSGG laser.³ Apart from the difference in laser wavelengths, the two laser sources also differ in the available pulse durations range. The Er,Cr:YSGG laser

is approximately limited to pulse durations above 400 μ s due to the slow Er-Cr relaxation times. Er:YAG lasers can operate at pulse durations under 100 μ s.⁴

Optimal parameters for the ablation of hard dental tissues, determined by wavelength and pulse duration, provide high ablation speed and minimize residual heat deposition in the tooth. A recent study compared ablation rates of the Er:YAG and Er,Cr:YSGG laser using an optical triangulation method.⁴⁻⁶ The Er:YAG laser was more effective in enamel by a factor of 1.6 and by a factor of 1.3 in dentin, in terms of ablation speed per

average laser power (in mm^3/W). This variation in the ablation efficacy was attributed to the differences in laser wavelength and pulse durations.

This study expands on the comparison between the two Erbium lasers to the remaining residual heat in the tooth following Erbium laser pulse ablation. The goal is to experimentally determine which conditions minimize undesirable thermal load on the tooth and thus approximate ideal “cold” optical drilling.

Numerous studies have simulated the temperature rise in tissues, or have used thermal cameras and thermocouples to measure temperature increase during laser irradiation.⁷⁻¹¹ However, there are only a few studies of the residual heat following each ablative laser pulse.^{12,13} Radiological measurements of temperatures during and immediately following the laser pulse in particular are obscured by the high temperatures of the re-irradiated ejected tissue and plasma formation, limiting the accuracy of the method to predominantly sub-ablative regimes.¹³ Fried et al determined residual heat deposition by measuring the temperature rise ratio induced by ablative and non-ablative laser pulses on the back side of bovine block “calorimeters”.¹² The measured residual heat deposition values varied between 25% and 70%, depending on the pulse duration and wavelength of the investigated laser systems. The study also indicated that residual heat deposition was reduced as laser pulses shortened.

This study determines residual heat from the thermal decay time of surface temperature. A thermal camera measures the temporal evolution of the tooth surface temperature following each laser pulse after the ablation plume has dispersed. This method is particularly suited for studying residual heat in ablative regimes. It can be assumed that the tissue surface temperature at the end of each pulse is always at the same approximate tissue-explosion temperature. Surface temperature decay time following each pulse depends on the final thickness of the heated tooth layer and therefore on the deposited heat during the pulse. The amount of remaining heat in the tissue after each laser pulse can thus be determined from the measured surface temperature decay time.

MATERIALS AND METHODS

The Er:YAG laser (AT Fidelis, Fotona) used in the study was fitted with a non-contact handpiece (R02, Fotona) with spotsize of 0.6 mm in focus. The Er,Cr:YSGG laser (Waterlase MD, Biolase) used was fitted with a fiber-tipped handpiece (Gold, Biolase) with 0.6-mm

spotsize. Comparisons between the two lasers were made using a range of available pulse duration settings for the two lasers: SSP (80 μs), MSP (150 μs) and SP (300 μs) for the AT Fidelis Er:YAG, and H (500-700 μs) and S (1200-1400 μs) for the Waterlase MD Er,Cr:YSGG.⁴ Water sprays were not used during the measurements.

We measured the above laser pulse durations for the two laser sources with the same photodiode at the R02 and Gold handpiece outputs. The temporal shapes of the pump flashlamp optical emissions were also measured by a diode detector. Figure 1 shows the flashlamp optical pulses and the resulting laser pulse durations of the Er: YAG laser system (MSP pulse mode), and of the Er,Cr:YSGG laser system (H and S pulse modes). Single pulse temporal evolutions without signal averaging are shown. Note that the measured laser pulse durations of the Er,Cr:YSGG laser system are much longer than the corresponding flashlamp pulse durations. For this reason, the pulse durations that are specified for the Er,Cr:YSGG laser system as 150 μs (H mode), and 700 μs (S mode) apply to the flashlamp pulse durations only. Due to the long population inversion lifetime of the Er,Cr:YSGG laser crystal, the generated laser pulses are considerably longer than the flashlamp pulses, and are in the shortest H pulse mode on the order of 500 to 700 μs , and for the longer S mode on the order of 1200 to 1400 μs .

A Flir ThermaCAM P45 thermal camera was fixed in position above the tooth surface and focused on the ablation site (Fig 2). The Er,Cr:YSGG fiber tip was positioned close to, but not in contact with, the tooth surface. The Er:YAG handpiece was positioned with the beam focused on the tooth surface.

Extracted premolars and molars that were stored in a 10% formalin solution immediately after extraction were randomly selected for the experiments. In each measurement, single laser pulses were delivered to different areas on the tooth to avoid cumulative tissue desiccation. Laser pulse energies (E_{pulse}) of $90 \text{ mJ} \pm 20\%$ were used to create laser fluences above the ablation threshold while keeping the ablated depth on the order of 10 μm or lower.⁴ Note that as explained further below, the laser pulse energy affects only the ablation depth, and not the final “boiling” temperature of the tooth. Thus the allowed $\pm 20\%$ variation in the laser energy level did not significantly influence the measured temperature decay curves.

The thermal camera was able to capture 50 images per second (one image every 20 ms) in quarter VGA resolution of 320x240 pixels. The image exposure time was approximately 5 milliseconds. The delay between

the camera rate and the laser pulses was adjusted so that the maximum measured temperature would fall within the first measurement image following a laser pulse. By doing so, the first measurement images were taken approximately 2.5 ms following a laser pulse. No alteration to the commercial laser devices was made. The lasers were fired as in normal operation by pressing the footswitch, and the camera image was recorded following the first emitted laser pulse out of the laser pulse train. This ensured that the temperature following a single pulse was measured and that there was no multiple laser pulse temperature buildup due to the high repetition rate of laser operation. Also, sufficient time was taken between measurements in order to allow the tooth to cool down to the ambient temperature before each recording. The energy of the first laser pulse out of the pulse train was also measured in order to avoid any error due to the possible energy drift within the laser pulse train. The energy was measured with an energymeter (Ophir Smarthead) at the corresponding R02 and Gold handpiece outputs.

RESULTS

Figure 3 shows that temperature decay is fastest in both dentin and enamel following MSP Er:YAG laser pulses. The difference in thermal decay times is most readily observed from the measured temperatures at 2.5 ms following a pulse, when the thermal diffusion effects are the most pronounced.

The initial temperature drop is a good indicator of the thermal decay time following a pulse, assuming that the initial surface temperature immediately after a pulse is equal to the tissue ablation temperature T_a (different for enamel and dentin) and thus independent of laser parameters. Lower measured temperatures indicate faster cooling and therefore shorter thermal decay times. Figure 4 shows the measured temperature differences, $\Delta T = T - T_0$, at 2.5 ms following a laser pulse under different experimental conditions. Here ΔT represents the temperature increase of the tooth above the initial average room temperature, T_0 , measured within a central 0.3-mm illuminated spot.

Figure 4 shows the measured temperatures are the lowest with the MSP Er:YAG laser pulses and therefore suggests the same for the thermal decay times. The measured temperatures are higher and thermal decay times longer in enamel than in dentin. At 100 mJ pulse energies, the differences between the measured thermal decay curves of the Er:YAG SSP, MSP and SP pulse duration settings lay within the experimental error

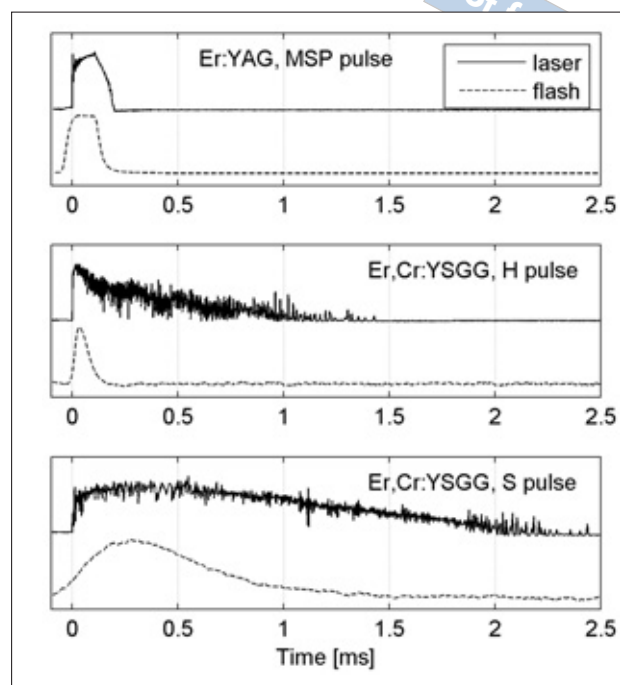


Fig 1 Measured temporal evolutions of the output laser radiation (full line), and flashlamp pump optical emission (dotted line) for Er:YAG laser system (Filedis AT, MSP pulse mode) and Er,Cr:YSGG laser system (Waterlase MD, H and S pulse mode).

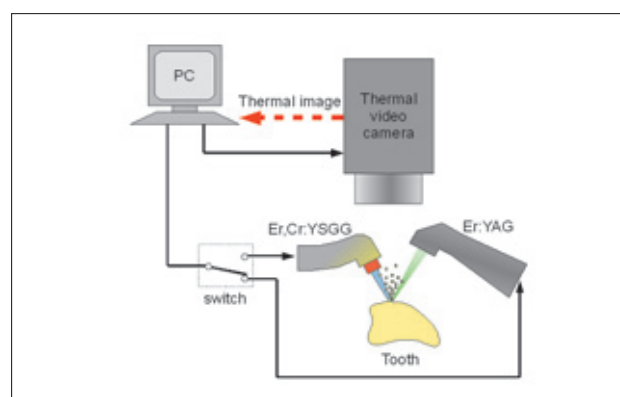


Fig 2 Experimental setup.

range. Measurements at higher pulse energies (not presented) revealed thermal decay to be faster for shorter Er:YAG pulse duration settings.

Analysis

The pulsed Erbium laser ablation mechanism of biological tissues is still not completely understood.¹⁴ Most researchers agree that the Erbium lasers' high ablation

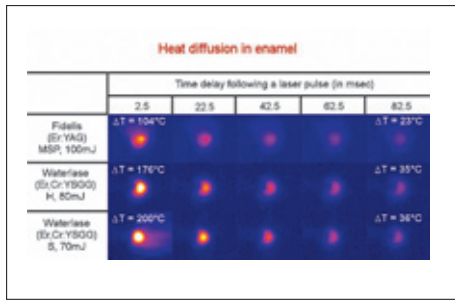
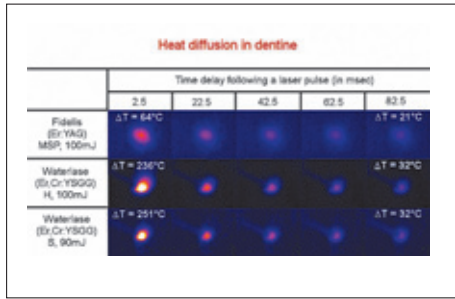


Fig 3 Typical thermal images of the irradiated tooth surface of the enamel (a) and dentin (b) at 2.5, 22.5, 42.5, 62.5 and 82.5 ms following a single laser pulse. The temperature difference, ΔT , represents the temperature increase above the initial average room temperature within a central 0.3-mm-diameter illuminated spot.

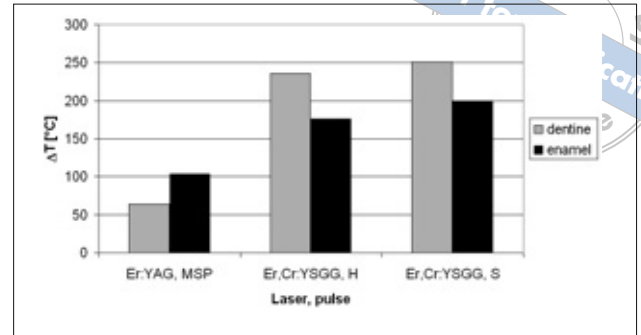


Fig 4 Enamel and dentin surface temperatures 2.5 ms after a laser pulse.

	Enamel	Dentin
ρ [kg/m ³]	2800	1960
λ [W/mK]	0.933	0.569
c_p [J/kgK]	711	1590
$D = \lambda/\rho c_p$ [m ² /s]	4.68×10^{-7}	1.83×10^{-7}

efficiency results from micro-explosions of water in overheated tissue in which their laser energy is predominantly absorbed.^{15,16}

The amount of heat that is deposited by a laser pulse on the tooth surface decreases with distance within the tissue. This is partially due to the exponential decrease of laser light intensity within tissue, as provided by

$$I = I_0 \exp(-\mu x), \tag{1}$$

where I_0 is the incident laser intensity and μ is the optical absorption coefficient of the tissue for the particular incident laser wavelength.

Heat distribution within the tissue is also created by conductive spreading of heat, ie, heat diffusion into the surrounding tissue. In the limit of a negligible optical absorption depth, the thermal distribution from a uniformly illuminated surface, for a duration time (t), is approximated by the Gaussian function^{17,21}

$$\Delta T = K \exp(-x^2/4Dt), \tag{2}$$

where D is the thermal diffusivity of the tissue, and K is a constant that depends on the laser and tissue parameters. The longer the pulse duration and the larger the thermal tissue diffusivity, the deeper the heat will spread away from the surface.

Ablation starts when the surface tissue is heated to the ablation temperature T_a . After that, and assuming a confined boiling model of laser ablation,¹⁶ surface temperature stops increasing and remains fixed at the “boiling” temperature T_a throughout the ablation process. However, the temperature distribution away from the surface continues to change during the laser pulse as the diffusion does not stop after the ablation threshold has been reached.

In what follows, we assume that the diffusion penetration depth, $d = \sqrt{4Dt}$, is larger than the optical penetration depth, $1/\mu$, and that the thermal distribution at the end of an ablative pulse can be approximated by:

$$\Delta T = (T_a - T_0) \exp(-x^2/d_R^2) \tag{3}$$

Here, the residual depth, d_R , represents the final depth of the heated layer, exactly at the end of a laser

Table 2 Measured temperature increase as a function of the elapsed time following an Erbium laser pulse

		Temperature increase ΔT [°C]			
Tissue	Laser	Time			
		2.5 ms	22.5 ms	42.5 ms	62.5 ms
Enamel	Er:YAG (MSP pulse)	110 ± 16	63 ± 15	46 ± 10	38 ± 11
	Er,Cr:YSGG (H pulse)	177 ± 23	85 ± 12	64 ± 18	43 ± 12
	Er,Cr:YSGG (S pulse)	204 ± 20	119 ± 22	71 ± 13	45 ± 7
	Dentin	Er:YAG (MSP pulse)	73 ± 11	48 ± 11	37 ± 7
	Er,Cr:YSGG (H pulse)	231 ± 27	77 ± 18	51 ± 12	39 ± 14
	Er,Cr:YSGG (S pulse)	246 ± 33	83 ± 20	56 ± 12	42 ± 13

pulse and represents a measure of the residual heat deposition. The thinner the layer, the smaller the amount of the deposited residual heat Q_{res} will be:

$$Q_{res} = A\rho c_p \int_0^{\infty} (T_a - T_0) \exp(-x^2/d_R^2) dx, \quad (4)$$

where A is the laser spot area, ρ the tissue density, and c_p the tissue heat capacity.

Heat continues to diffuse into the tissue and surface temperature starts decreasing below T_a , after the laser pulse has ended. Here, we ignore the much slower convective surface cooling into the surrounding air. Assuming a thermal distribution at the end of a laser pulse to be as described in (3), the temporal surface temperature evolution, T , following a laser pulse can be calculated using a one-dimensional diffusion equation^{17,21}:

$$\frac{\rho c}{\lambda} \frac{\partial T}{\partial t} = \frac{\partial^2 T}{\partial x^2} \quad (5)$$

The one dimensional diffusion equation is taken to be a good approximation since the laser spot diameter is much larger than the diffusion depth. Alternatively, the initial T_a and d_R can be determined from the measured surface temperature decay by fitting the calculated temperature decay curves to the measured results.

The parameters as shown in Table 1 were used in the diffusion model.¹⁹

The measured values for temperature increase ΔT following an Erbium pulse in dentin and enamel, averaged over five recordings, are shown in Table 2.

Figures 5 and 6 show the measured temperature decay data from Table 2, together with the best numerical fit to the diffusion equation (Eq 5).

The best fit to all measurements is obtained by taking ablative temperatures, T_a , of $600^\circ\text{C} \pm 50^\circ\text{C}$ for enamel, and $500^\circ\text{C} \pm 50^\circ\text{C}$ for dentin. Figure 7 presents the obtained residual depths of the deposited heat calculated from data in Figs 5 and 6.

The corresponding values of the residual heat as obtained from (Eq 4) are shown in Fig 8.

DISCUSSION

A water spray was not used during the measurements as the goal was to determine the residual heat deposition, and not the actual temperature decay times under clinical conditions. Water cooling of the irradiated tooth surface during the laser pulse is not substantial, since the water layer is vaporized during the ablative stage and an optical "hole" is made in the layer.¹⁸ Control measurements in which temperature decay curves were obtained following an Erbium laser pulse with a

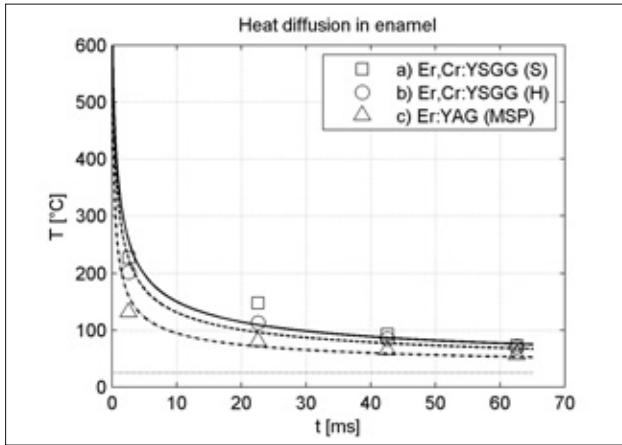


Fig 5 Enamel surface temperature decay following an a) Er,Cr:YSGG laser S pulse; b) Er,Cr:YSGG laser H pulse; and c) Er:YAG laser MSP pulse. Lines represent a numerical fit to Eq. (5) where the best fit was obtained with diffusion constants d_R of (a) 30 μm ; (b) 25 μm , and (c) 15 μm , respectively. The horizontal dotted line represents the initial ambient temperature T_0 .

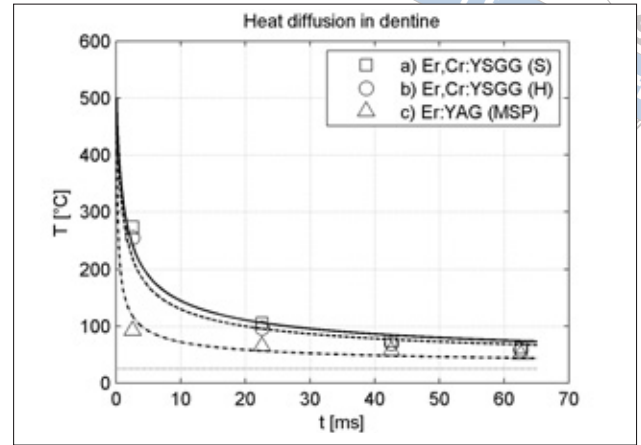


Fig 6 Dentin surface temperature decay following an a) Er,Cr:YSGG laser S pulse; b) Er,Cr:YSGG laser H pulse; and c) Er:YAG laser MSP pulse. Lines represent a numerical fit to Eq. (5) where the best fit was obtained with diffusion constants d_R of (a) 22 μm ; (b) 19 μm , and (c) 7 μm , respectively. The horizontal dotted line represents the initial ambient temperature T_0 .

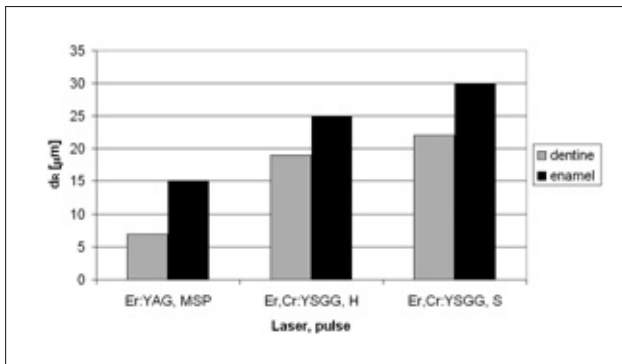


Fig 7 Calculated residual depths d_R in dentin and enamel, obtained from the thermal decay measurements.

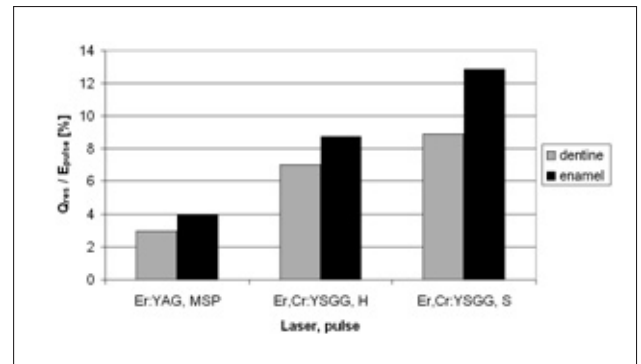


Fig 8 Residual heat Q_{res} as a percentage of the laser pulse energy E_{pulse} .

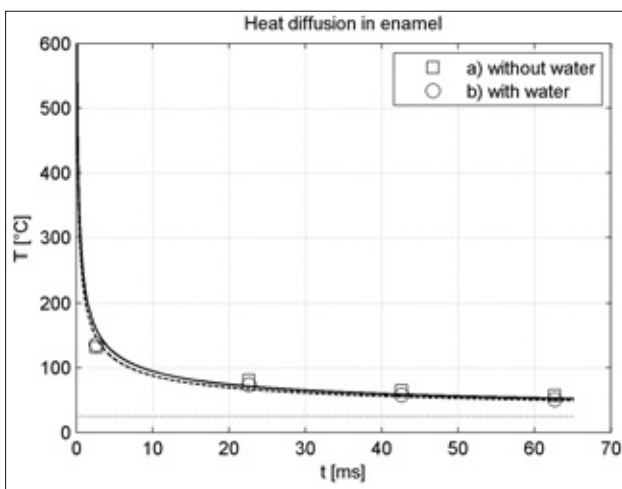


Fig 9 Comparison of temperature decays following an Er:YAG MSP laser pulse (a) without and (b) with water layer on the enamel surface. The calculated diffusion constant d_R was estimated to be (a) 15 μm and (b) 13 μm , respectively. Horizontal dotted line represents the initial ambient temperature T_0 .

water drop deposited on the tooth, prior to laser irradiation, confirmed this. For either of the laser sources, the water layer did not affect the temperature decay values by more than 10%, which was within the temperature measurement error. As an example, Fig 9 shows the measured temperature decay curves for the MSP Er:YAG laser pulses, with and without the water layer.

The absorption coefficients μ for the Er:YAG laser are approximately 150 mm^{-1} in enamel, and 200 mm^{-1} in dentin.^{15,20} The corresponding absorption coefficients for the Er,Cr:YSGG laser are approximately three times lower. The Er:YAG laser wavelength thus penetrates approximately $7 \mu\text{m}$ in enamel, and $5 \mu\text{m}$ in dentin (Eq 1). The Er,Cr:YSGG laser wavelength penetrates deeper: $21 \mu\text{m}$ in enamel, and $15 \mu\text{m}$ in dentin. Comparison shows that these optical penetration depths are smaller than the determined residual depths, d_R , under most experimental conditions and in agreement with the assumption of a diffusion-dominated temperature distribution (Eq 3). Also note that the absorption of hard tissue may change during laser irradiation. Thus it has been suggested that the water absorption might shift at high laser energies towards shorter wavelengths.¹⁴ This would make the absorption difference between the Er:YAG and Er,Cr:YSGG wavelengths smaller, and the application of the same temperature distribution model for both laser sources more valid.

The actual temperature distribution, especially at shorter pulse durations, is undoubtedly a combination of the optical exponential and diffusive Gaussian function. However, the exact shape of the thermal distribution curve does not have a significant effect on the numerical fitting and the residual depths d_R , obtained by assuming Gaussian distribution. The residual depths, as shown in Fig 7, can therefore be taken as a meaningful measure of the thickness of the residual thermal layer and therefore of the residual deposited heat for all considered laser parameters.

At high energies and short pulse durations (ie, at high laser pulse powers), the ablation speed may become comparable to the rate at which heat diffuses into the tissue.¹⁵ Towards higher laser pulse powers, the thermally affected tissue layer is thus reduced by the ablation of the preheated tissue and is increasingly confined only to the directly heated volume within the optical penetration depth. This effect has been experimentally measured by Fried et al, who observed a gradual reduction in the residual heat towards higher laser fluences.¹² This also applies to our experiment, where estimated ablation depths at the fluence used

were on the order of $10 \mu\text{m}$,⁴ possibly significantly reducing the diffusion-mediated thermal layer. The residual depths, d_R , obtained in our study thus apply only to the specific fluences used in our experiment (approximately 35 J/cm^2).

CONCLUSIONS

The amount of residual heat that remains in hard dental tissues after Erbium laser irradiation has been obtained from the measured rates of the surface temperature decay. The measurements reveal a much faster temperature decay following the Er:YAG laser compared to the Er,Cr:YSGG laser, indicating smaller depth of the remaining heated layer. This is attributed to the shorter pulse duration and smaller optical penetration depth of the Er:YAG laser. For both lasers, the measured residual heat is larger in enamel than in dentin. At pulse energies of 100 mJ, the amount of unwanted residual heat that remains deposited in the tooth is for the H mode Er,Cr:YSGG laser larger by a factor of more than two, and for the S mode Er,Cr:YSGG laser larger by a factor of more than three, compared to the deposited heat with the MSP mode Er:YAG laser. For Er,Cr:YSGG lasers, a larger share of the total laser energy remains in the tooth in the form of heat. This contributes to the reported lower ablation efficacy of Er,Cr:YSGG lasers.⁴

ACKNOWLEDGMENTS

Co-authors Dr. Matjaz Lukac and Dr. Marko Marincek are affiliated with Fotona d.d.

REFERENCES

1. Hibst R. Lasers for Caries Removal and Cavity Preparation: State of the Art and Future Directions. *J Oral Laser Appl* 2002;2:203-211.
2. Lukac M, Marincek M, Grad L. Super VSP Er:YAG Pulses for Fast and Precise Cavity Preparation. *J Oral Laser Appl* 2004;4:171-173.
3. Meister J, Franzen R, Forner K, Grebe H, Stanzel S, Lampert F, Apel C. Influence of the water content in dental enamel and dentin on ablation with erbium YAG and erbium YSGG lasers. *J Biomed Opt* 2006 11:034030:1-7.
4. Perhavec T, Diaci J. Comparison of Er:YAG and Er,Cr:YSGG dental lasers. *J Oral Laser Appl* 2008;8:87-94.
5. Perhavec T, Gorkiä A, Braäun D, Diaci J. A method for rapid measurement of laser ablation rate of hard dental tissue. *Optics and Laser Technology* 2009;41:397-402.

6. Diaci J. Laser Profilometry for the Characterization of Craters Produced in Hard Dental Tissues by Er:YAG and Er,Cr:YSGG Lasers. *J Laser Health Academy* 2008;2.
7. Zuerlin MJ, Fried D, Seka W, Featherstone JDB. Modelling thermal emission in dental enamel induced by 9-11 μm laser light. *Appl Surf Science* 1989;127-129:863-868.
8. Armengol V, Jean A, Marion D. Temperature rise during Er:YAG and Nd:YAP laser ablation of dentin. *J Endod* 2000;26:138-141.
9. Fried D, Visuri SR, Featherstone JDB, Walsh JT, Seka W, Glens RE, McCormack SM, Wigdor HA. Infrared radiometry of dental enamel during Er:YAG and Er:YSGG laser irradiation. *J Biomedical Opt* 1996;1:455-465.
10. Venugopalan V, Nishioka NS, Mikic BB. Thermodynamic response of soft biological tissues to pulsed infrared laser irradiation. *Biophysical J* 1996;70:2981-2993.
11. Harris DB, Fried D, Reinisch L, Bell T, Chachter D, From L, Burkart J. Eyelid resurfacing. *Lasers in Surg. Med* 1999;25:107-122.
12. Fried D, Ragadio J, Champion A. Residual heat deposition in dental enamel during IR laser ablation at 2.79, 2.94, 9.6, and 10.6 μm . *Lasers Surg Med* 2001;29:221-229.
13. Neev J, DaSilva LB, Feit MD, Perry MD, Rubenchik AM, Stuart BC. Ultrashort pulse lasers for hard tissue ablation. *IEEE J Selected Topics Quant Electr* 1996;2:790-808.
14. Vogel V, Venugopalan. Mechanisms of Pulsed Laser Ablation of Biological Tissues. *Chem Rev* 2003;103:577-644.
15. Majaron D, Sustersic M; Lukac U, Skaleric N, Funduk. Heat diffusion and debris screening in Er:YAG laser ablation of hard biological tissues. *Appl Phys B* 1998;66:1-9.
16. Majaron P, Plestenjak M, Lukac. Thermo-mechanical laser ablation of soft tissue: modeling the micro-explosions. *Appl Phys B* 1999;69:71-80.
17. Cox B. Introduction to Laser-Tissue Interactions, PHAS 4886 Optics in Medicine 2007;October:1-61.
18. Forrer M, Frenz M, Romano V, Weber HP. Channel propagation in water and gelatine by a free-running erbium laser. *J Appl Phys* 1993;74:720-727.
19. Brown WS, Dewey WA, Jacobs HR. Thermal properties of teeth. *J Dent Res* 1970;49:752-755.
20. Ivanov B, Hakimian AM, Peavy GM, Haglund RF. Mid-infrared laser ablation of hardbiocomposite material: mechanistic studies of pulse duration and Interface effects. *Appl Surf Sci* 2003;208-209:77-84.
21. Niemz MH, Laser-Tissue Interactions: Fundamentals and Applications, 2nd edition. Berlin: Springer, 2002:58-85.

Contact address: Tadej Perhavec, University of Ljubljana, Faculty of Mechanical Engineering, Aškerčeva 6, 1000 Ljubljana, Slovenia. Fax: + 386 1 5009 200.
e-mail: perhavec.tadej@gmail.com